Adaptive Iterative Learning Control for Subway Trains Using Multiple-Point-Mass Dynamic Model Under Speed Constraint

Genfeng Liu and Zhongsheng Hou, *Fellow, IEEE*

***Abstract*—In this paper, a new adaptive iterative learning control method (AILC) is presented for speed and position tracking of a subway train using multiple-point-mass dynamic model. A composite energy function technique is utilized to obtain the asymptotic convergence of tracking error in the iteration axis for the proposed controller for subway trains. Then a speed constraint adaptive iterative learning control algorithm (CAILC) is designed to avoid over speed, derailment and collision of the subway train for the subway train over-speed protection. Finally, two simulation examples are given for the subway train system to show the effectiveness of theoretical studies.**

***Index Terms*—Subway train, speed constraint, multiple-point-mass dynamic model, adaptive iterative learning control (AILC), tracking control, barrier composite energy function (BCEF).**

I. Introduction

SUBWAY has drawn widespread attention and developed rapidly in recent years, because of its high carrying capacity, reliability, safety, small departure interval and fixed schedule. Subway becomes an indispensable transportation tool for alleviating the transportation pressure in metropolises [1]. With the rapid development of city subway, it is urgent demand to improve operation efficiency of the subway train. In such circumstance, the subway train operation control technology becomes a hot topic in control theory research community. The automatic train control (ATC) system is a key module to guarantee safe operation of subway trains. ATC contains automatic train operation (ATO), automatic train protection (ATP) and automatic train supervision (ATS). Wherein the ATO is a vital subsystem which conducts all phases of subway train operation, for instance, stopping operation, traction and braking control, etc. [2], [3].

The design of subway train ATO consists of two stages. The first stage is to generate the offline desired speed profile [4]–[10]. In [4], for a given route, an optimal control method is designed according to minimum energy consumption. In [5], optimal train trajectories are established by a fitness function. Based on a distance-based train trajectory searching model, the ant colony optimization algorithm, genetic algorithm and dynamic programming are proposed for optimum train speed trajectory in [6]. In [7], the pseudospectral technique and mixed integer linear programming algorithm are presented to deal with the optimal trajectory planning issue for subway trains. In order to optimize the speed profile of subway trains, an integrated method is proposed in [8], and further in [9], the integrated law is used to obtain the globally optimal operation schedule for subway trains so as to achieve better control performance. In [10], a dynamic programming method is investigated to improve train speed profiles with reduced energy consumption.

Under desired speed profile pre-specified, the main task of ATO is speed regulation. The second stage is to execute automatic subway train control strategy to track the desired speed profile. Various intelligent control methods are studied and applied for single train including genetic algorithm [11], expert system method and reinforcement learning law [12], PID controller [3], [13], multi-modal fuzzy PID control algorithm with neural networks [14], predictive fuzzy control [15], model predictive control [16], event-based control law [17], and multi-objective system optimization of metro trains [18], etc. With the increasing requirement of multiple trains' operation safety, the cooperative control for multiple trains has attracted the attention. An energy-saving based cooperative train control method is studied in [19]. In [20], for multiple high-speed trains with actuator faults and disturbances, two adaptive fuzzy control approaches are proposed to guarantee the errors bounded tracking and string stability. In [21], for high-speed trains with input saturation, a CNN based distributed adaptive control method with sliding mode technique is investigated. In [22], considering mismatch input quantization, unknown actuator deadzone and disturbances, a PID sliding mode control scheme is presented for heterogeneous vehicles which ensures the spacing error bounded tracking and string stability. All these control methods mentioned above are feedback control strategies in time domain, which can ensure tracking error convergence as the time approaches infinity. However, the theoretical control performance when time goes to infinity for subway trains cannot be expected because it is operating in a finite time interval. Meanwhile, the typical repetitive

Manuscript received November 4, 2018; revised June 26, 2019 and October 24, 2019; accepted January 23, 2020. This work was supported in part by the National Natural Science Foundation of China under Grant 61833001 and Grant 61433002, and in part by the Beijing Natural Science Foundation under Grant L161007. The Associate Editor for this article was R. Goverde. *(Corresponding author: Genfeng Liu.)*

Genfeng Liu is with the Advanced Control Systems Laboratory, School of Electronic and Information Engineering, Beijing Jiaotong University, Beijing 100044, China (e-mail: 16111050@bjtu.edu.cn).

Zhongsheng Hou was with the Advanced Control Systems Lab, School of Electronic and Information Engineering, Beijing Jiaotong University, Beijing 100044, China. He is now with the School of Automation, Qingdao University, Qingdao 266071, China (e-mail: zhshhou@bjtu.edu.cn; zshou@qdu.edu.cn).

Digital Object Identifier 10.1109/TITS.2020.2970000

operation pattern of a subway train cannot be utilized. As a result, its performance cannot be improved as the times of the subway train operation increase. It is well known that the subway train has a very prominent repetitive operation feature, which implies that a subway train runs from one station to the next in accordance with its operation timetable every day, and its operating environment and control task keep also unchanged. Fortunately, the iterative learning control (ILC) method [23]–[27], which targets to guarantee the tracking error of a train operation speed profile from the very begin to the very end of the train operation interval to the desired speed profile goes to zero as the iteration number goes to infinity, is the most suitable control method among the various modern control methods since it is the only one which is specifically proposed for the control issue for the repeated operating system in a finite time interval, and the ILC law design only requires a small amount of system model prior knowledge and it does not needs the precise system model. In [28], for train station stop problem, a terminal iterative learning control algorithm was first proposed which can ensure precise train stopping. In [29], considering trains over speed protection and safety, a coordinated iterative learning control law was designed. For high-speed train's operation control, an adaptive iterative learning control (AILC) algorithm was investigated to solve the issue of unknown speed delays and control input saturations in [30]. In [31], a novel norm optimal iterative learning control scheme was proposed for high-speed trains which ensures 2-norm convergence of the train speed tracking error.

Most of aforementioned control schemes were developed and applied based on the single-point-mass dynamic model. However, a subway train usually consists of many vehicles, which are connected with elastic couplers. It is generally a type of power distributed driving system. Based on the above mention consideration, it is more reasonable to treat the subway train system as a multiple-point-mass object, and the multiple-point-mass dynamic model can supply more variables to accurately describe the overall dynamics of the subway train system. Therefore, to improve the tracking precision of the subway train, it is worthy to build the multiple-point-mass dynamic model of a subway train first and then to design subway train controller.

To the best knowledge of the authors, however, very few works exist on automatic train control on the multiple-point-mass dynamic model of a subway train. The main works could be found in [32]–[35]. By linearizing the nonlinear multiple-point-mass dynamic model of train system, a mixed H_2/H_∞ cruise control scheme is developed for high-speed trains in [32]. In [33], using the nonlinear multiple-point-mass dynamic model of the train, a speed regulation problem is investigated for heavy haul trains. In [34], based on hybrid model reference, a novel adaptive sliding mode control approach is presented for automatic train operation. In [35], a computationally inexpensive tracking control of high-speed trains with traction/braking saturation is proposed which can achieve uniformly ultimately bounded of tracking error. All of these control methods for trains are based on feedback control approaches in the time domain which indicates that the typical repetitive pattern of the train system is not fully exploited. Based on the feedback control scheme, no matter how many times the subway train operates, the subway train control system has the same control performance that cannot be improved as the number of operation increases.

For the operation safety of the mass transport subway train, over speed can cause derailment and collision of the subway train. Hence, speed constraint is an important issue to ensure the safe and reliable operation of the subway train. In the above mentioned control schemes of the train operation, speed constraint is not taken into account and is left to be handled by the onboard ATP hardware system, which may be affected by unsafe factors due to hardware fault. Considering speed constraint, some ATO algorithms for trains have also attracted attention [29], [36]. But they are all the results based on the single-point-mass model.

Inspired by the above observations, this paper investigates an adaptive iterative learning control method with speed constraint by using repetitive pattern of the subway train and multiple-point-mass dynamic model to improve gradually control performance as the iteration number goes to infinity.

The major contributions of this paper are as follows.

i) Applying iterative learning control theory and the multiple-point-mass dynamic model of the subway train, a novel adaptive iterative learning control algorithm is proposed to improve the speed and position tracking performance of subway trains. Moreover, in order to avoid over speed, derailment and collision of the subway train, a speed constrained adaptive learning control (CAILC) is also designed.
ii) The convergence of the subway train speed and position tracking error is rigorously analyzed, which will ensure safe, reliable and efficient operation of subway trains. Finally, the results of subway train simulation verify the effectiveness of theoretical studies.
iii) Based on the multiple-point-mass dynamic model, the proposed control method enables the subway train to run more safely and reliably than existing ILC methods, because the in-train forces between each vehicles, dynamics of each vehicle of the subway train and speed constraint are all considered for controller design.

The remainder of this paper is organized as follows. In Section II, the multiple-point-mass dynamic model of the subway train is introduced and the tracking problem is formulated. Section III conducts design and analysis of a new adaptive learning control algorithm for the subway train speed and positon tracking. In Section IV, such a tracking problem under speed constraint is considered, and a speed constraint adaptive iterative learning control (CAILC) is investigated. In Section V, optimal traction/braking force distribution is studied. Section VI is the subway train simulation examples to verify the effectiveness of theoretical studies. Then, in Section VII, some conclusions are summarized for this paper.

II. Subway Train System Model and Problem Formulation

A. Subway Train System Multiple-Point-Mass Model

In terms of Newton's law of mechanics, the following dynamic model for each vehicle is described as [33], [35]

$$m^{(k)}\ddot{y}^{(k)}(t)=\mu^{(k)}F^{(k)}(t)-f^{(k)}(t)+f^{in_{(k-1)}}(t)-f^{in_{(k)}}(t) \quad (1)$$

where t denotes the time, $k=1,2,\cdots,n$ in brackets is the number of vehicles, $m^{(k)}$ denotes the mass of the k-th vehicle. $y^{(k)}(t)$ is the distance between the center of the k-th vehicle and the zero reference point, which can see Fig. 1. $\dot{y}^{(k)}(t)$ and $\ddot{y}^{(k)}(t)$ are the speed and acceleration for the k-th vehicle. $\mu^{(k)}$ denotes a known distribution constant that deals with the traction/braking effort of the k-th vehicle. $F^{(k)}(t)$ indicates the traction/braking force of the k-th vehicle, i.e. the control input of the system. $f^{(k)}(t)$ denotes the resistance for the k-th vehicle. $f^{in_{(k)}}(t)$ stands for the in-train force among the adjacent vehicles.

During a subway train's operation on the track, the distance between two adjacent vehicles $y^{(k+1)}(t)-y^{(k)}(t)$ is established by $s^{(k)}(t)$, $\vartheta^{(k)}$ and half of vehicle length l, wherein $s^{(k)}(t)$ denotes the absolute compression or extension length for the k-th elastic coupler. $\vartheta^{(k)}$ is a constant which indicates the length of the elastic coupler that is not deformed.

From Fig.1, it becomes $s^{(k)}(t)=y^{(k+1)}(t)-y^{(k)}(t)-l-l-\vartheta^{(k)}$, and $\dot{s}^{(k)}(t)=\dot{y}^{(k+1)}(t)-\dot{y}^{(k)}(t)$. Therefore, the speed and acceleration of each vehicle are $\dot{y}^{(k)}(t)=\dot{y}^{(1)}(t)+\sum_{j=1}^{k-1}\dot{s}^{(j)}(t)$ and $\ddot{y}^{(k)}(t)=\ddot{y}^{(1)}(t)+\sum_{j=1}^{k-1}\ddot{s}^{(j)}(t)$.

Taking into account all vehicles of a subway train and the in-train forces between them and combined with (1), the multiple-point-mass dynamic model of subway train system is derived as follows.

$$\begin{bmatrix} m^{(1)} & & & \\ & m^{(2)} & & \\ & & \ddots & \\ & & & m^{(n)} \end{bmatrix}\begin{bmatrix} \ddot{y}^{(1)}(t) \\ \ddot{y}^{(2)}(t) \\ \vdots \\ \ddot{y}^{(n)}(t) \end{bmatrix} = \begin{bmatrix} \mu^{(1)} & & & \\ & \mu^{(2)} & & \\ & & \ddots & \\ & & & \mu^{(n)} \end{bmatrix}\begin{bmatrix} F^{(1)}(t) \\ F^{(2)}(t) \\ \vdots \\ F^{(n)}(t) \end{bmatrix} - \begin{bmatrix} f^{(1)}(t) \\ f^{(2)}(t) \\ \vdots \\ f^{(n)}(t) \end{bmatrix} + \begin{bmatrix} f^{in_{(0)}}(t) \\ f^{in_{(1)}}(t) \\ \vdots \\ f^{in_{(n-1)}}(t) \end{bmatrix} - \begin{bmatrix} f^{in_{(1)}}(t) \\ f^{in_{(2)}}(t) \\ \vdots \\ f^{in_{(n)}}(t) \end{bmatrix} \quad (2)$$

Since there are no in-train forces for the first and the last vehicles, $f^{in_{(0)}}(t)=0$, $f^{in_{(n)}}(t)=0$.

The resistance of the subway train system is given by

$$f^{(k)}(t)=a^{(k)}(t)+b^{(k)}(t)\dot{y}^{(k)}(t)+c^{(k)}(t)(\dot{y}^{(k)}(t))^2+f^{add_{(k)}}(t) \quad (3)$$

where $a^{(k)}(t)$, $b^{(k)}(t)$ and $c^{(k)}(t)$ stand for unknown time-dependent resistance coefficients of the k-th vehicle. $f^{add_{(k)}}(t)$ is the bounded additional resistance for the k-th vehicle including tunnel resistance, gradient resistance and curve resistance.

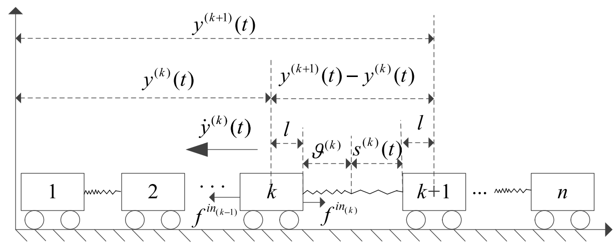

Fig. 1. A subway train with n vehicles connected with elastic couplers.

From (2), it further leads to

$$\begin{aligned} m^{(1)}\ddot{y}^{(1)}(t) &= \mu^{(1)}F^{(1)}(t)-f^{(1)}(t)-f^{in_{(1)}}(t) \\ &\vdots \\ m^{(n)}\ddot{y}^{(1)}(t) &= \mu^{(n)}F^{(n)}(t)-f^{(n)}(t)+f^{in_{(n-1)}}(t) \\ &\quad -m^{(n)}\sum_{j=1}^{n-1}\ddot{s}^{(j)}(t) \end{aligned} \quad (4)$$

where $y^{(1)}$ is the position of the leading vehicle.

By summing all terms on both sides of the equation (4), a compact form for (4) can be expressed as

$$\begin{aligned} &(m^{(1)}+m^{(2)}+\cdots+m^{(n)})\ddot{y}^{(1)}(t) \\ &= \left[\mu^{(1)}\ \mu^{(2)}\ \cdots\ \mu^{(n)}\right]\begin{bmatrix} F^{(1)}(t) \\ F^{(2)}(t) \\ \vdots \\ F^{(n)}(t) \end{bmatrix} - \sum_{k=1}^{n} f^{(k)}(t) \\ &\quad -\ddot{s}^{(1)}(t)\sum_{k=2}^{n}m^{(k)}-\ddot{s}^{(2)}(t)\sum_{k=3}^{n}m^{(k)}-\cdots-\ddot{s}^{(n-1)}(t)m^{(n)} \end{aligned} \quad (5)$$

which means

$$\begin{aligned} M\ddot{y}^{(1)}(t) &= \left[\mu^{(1)}\ \ \mu^{(2)}\ \ \cdots\ \ \mu^{(n)}\right]\begin{bmatrix} F^{(1)}(t) \\ F^{(2)}(t) \\ \vdots \\ F^{(n)}(t) \end{bmatrix} - F_D(t) - F_K(t) \\ &= \boldsymbol{\Upsilon}\boldsymbol{F}(t)-F_D(t)-F_K(t) \end{aligned} \quad (6)$$

where $\boldsymbol{\Upsilon}=[\mu^{(1)},\mu^{(2)},\cdots,\mu^{(n)}]$ is a known vector consisting of distribution constants. $\boldsymbol{F}(t)=[F^{(1)}(t),F^{(2)}(t),\cdots,F^{(n)}(t)]^T$ denotes a traction/braking force vector. $F_D(t)=\sum_{k=1}^{n}f^{(k)}(t)$, $F_K(t)=\sum_{k=1}^{n-1}(\ddot{s}^{(k)}(t)\sum_{j=k+1}^{n}m^{(j)})$, $M=\sum_{k=1}^{n}m^{(k)}$.

To facilitate the control scheme design and analysis, we apply x to replace the position $y^{(1)}$ of the leading vehicle. In terms of (3)-(6), we can obtain

$$M\ddot{x}(t)=\boldsymbol{\Upsilon}\boldsymbol{F}(t)+\boldsymbol{\Xi}^T(t)\boldsymbol{\xi}(t) \quad (7)$$

where $\boldsymbol{\Xi}(t)=[R_1(t),R_2(t),R_3(t)]^T$ represents a unknown bounded parameters vector. $\boldsymbol{\xi}(t)=[-1,-\dot{x}(t),-\dot{x}^2(t)]^T$ indicates a known vector valued function which satisfies the local Lipschitz continuity conditions[37], [38] for velocity. That is, for a convex subset D and constant T_D, $t\in[0,T_D]$,

$\dot{x}_1, \dot{x}_2 \in D$, there exists a constant $L_\xi \geq 0$, such that $\|\xi_1 - \xi_2\| \leq L_\xi |\dot{x}_1 - \dot{x}_2|$.

The unknown parameters are

$$\begin{aligned}
R_1(t) &= \sum_{k=1}^{n}\left(b^{(k)}(t)\sum_{j=1}^{k-1}\dot{s}^{(j)}(t)\right)+\sum_{k=1}^{n}\left(c^{(k)}(t)\left(\sum_{j=1}^{k-1}\dot{s}^{(j)}(t)\right)\right)^2\\
&\quad+\sum_{k=1}^{n} f^{add(k)}(t)+\sum_{k=1}^{n-1}\left(\ddot{s}^{(k)}(t)\sum_{j=k+1}^{n} m^{(j)}\right)+\sum_{k=1}^{n} a^{(k)}(t)\\
R_2(t) &= 2\sum_{k=1}^{n}\left(c^{(k)}(t)\sum_{j=1}^{k-1}\dot{s}^{(j)}(t)\right)+\sum_{k=1}^{n} b^{(k)}(t)\\
R_3(t) &= \sum_{k=1}^{n} c^{(k)}(t)
\end{aligned} \tag{8}$$

Remark 1: Contrasted with the traditional single-point-mass model, the multiple-point-mass of the subway train contains dynamics of trailers and power vehicles, which describes the dynamics of each vehicle with the different resistances and is more accurate and practical for controller design of the subway train system. Equation (8) involves unknown time-varying resistances of each vehicle and in-train forces that are reflected in the absolute extension or compression length $s^{(k)}(t)$ and its derivatives.

B. Problem Formulation

The subway train runs repetitively on a track every day according to their operation diagrams in a finite time interval from one station to the next. Considering the characteristics of the subway train operation, the subway train system (7) can be described in a repeated manner with iteration index i.

$$M\ddot{x}_i(t) = \boldsymbol{\Upsilon} \boldsymbol{F}_i(t) + \boldsymbol{\Xi}^T(t)\xi_i(t) \tag{9}$$

where $x_i(t)$ and $\dot{x}_i(t)$ denote the output position and speed of the subway train at the i-th iteration.

For convenience, we define $u_i(t) = \boldsymbol{\Upsilon} \boldsymbol{F}_i(t)$, which is the traction/braking force of the subway train. The controller design process is to design $u_i(t)$ and then to conduct optimal distribution of the subway train traction/braking force $u_i(t)$ for each vehicle in Section V.

The control objective is to design a controller $\boldsymbol{F}_i(t)$ for subway train system (9), such that the position tracking error $e_i(t) = x_i(t) - x_r(t)$ and speed tracking error $\dot{e}_i(t) = \dot{x}_i(t) - \dot{x}_r(t)$ converge to zero as the iteration number i goes to infinity. $x_r(t)$ and $\dot{x}_r(t)$ are the bounded desired position and speed trajectory that are predesigned.

III. AILC Design and Convergence Analysis

For the convenience of controller design and analysis, an augmented error is introduced.

$$\delta_i(t) = \alpha e_i(t) + \dot{e}_i(t) \tag{10}$$

where α denotes a positive parameter.

According to (9) and (10), the augmented error dynamics of the subway train system can be obtained.

$$M\dot{\delta}_i(t) = u_i(t) + \boldsymbol{\Xi}^T(t)\boldsymbol{\xi}_i(t) - M\ddot{x}_r(t) + M\alpha\dot{e}_i(t) \tag{11}$$

Assumption 1: The identical initial conditions i.e., $x_i(0) = x_r(0) = 0$, $\dot{x}_i(0) = \dot{x}_r(0) = 0$ are satisfied.

Remark 2: The above assumption imposed on the subway train system is reasonable and acceptable, since the subway train departs from the same station with zero initial speed every operation.

The adaptive iterative learning control algorithm (AILC) for subway trains is presented as

$$u_i(t) = -\hat{\boldsymbol{\Xi}}_i^T(t)\xi_i(t) + M\ddot{x}_r(t) - M\alpha\dot{e}_i(t) - \beta\delta_i(t) \tag{12}$$

where β is a feedback gain.

The parameter updating law for $\hat{\boldsymbol{\Xi}}_i(t)$ is

$$\hat{\boldsymbol{\Xi}}_i(t) = \hat{\boldsymbol{\Xi}}_{i-1}(t) + \boldsymbol{\Gamma}\delta_i(t)\xi_i(t),\ \hat{\boldsymbol{\Xi}}_{-1}(t) = 0 \tag{13}$$

where $\boldsymbol{\Gamma}$ denotes the learning gain diagonal matrix.

Remark 3: Control law (12) consists of two parts, i.e. compensation term $-\hat{\boldsymbol{\Xi}}_i^T(t)\boldsymbol{\xi}_i(t) + M\ddot{x}_r(t)$ and feedback part $-M\alpha\dot{e}_i(t) - \beta\delta_i(t)$. Compensation term can improve the tracking accuracy of the system. The feedback term can stabilize the subway train system and increase the robustness of the onboard train control system. $\ddot{x}_r(t)$ is the known desired acceleration for controller design, which is predesigned by designer. In practice, the actual acceleration of the subway train can be obtained by accelerometer, or the acceleration can be measured by differentiating the speed, which can be measured by the speed sensor.

The convergence of the proposed control algorithm for the subway train is summarized in the theorem 1.

Theorem 1: Considering the subway train system (9) satisfying assumption 1, the adaptive iterative learning control scheme (12) and the parameter updating algorithm (13) can ensure that the speed and position tracking error asymptotically converges to zero in a pointwise manner when the iteration number i goes to infinity.

Proof: To obtain the learning property of the proposed AILC for the subway train system, a composite energy function (CEF) is constructed as

$$\begin{aligned}
E_i(t) &= \frac{1}{2}M\delta_i^2(t) + \frac{1}{2}\int_0^t \tilde{\boldsymbol{\Xi}}_i^T(\tau)\boldsymbol{\Gamma}^{-1}\tilde{\boldsymbol{\Xi}}_i(\tau)d\tau\\
&= V_{\delta,i}(t) + V_{\Xi,i}(t)
\end{aligned} \tag{14}$$

where $V_{\delta,i}(t) = M\delta_i^2(t)/2$, $V_{\Xi,i}(t) = \int_0^t \tilde{\Xi}_i^T(\tau)\boldsymbol{\Gamma}^{-1}\tilde{\Xi}_i(\tau) d\tau/2$.

The proof of theorem 1 contains three parts. Part A is decreasing property of the CEF. Part B is the boundness of $E_0(t)$ and Part C proves the pointwise convergence of tracking error.

Part A: Non-increasing property of the CEF

According to (14), one gets

$$\begin{aligned}
\Delta E_i(t) &= E_i(t) - E_{i-1}(t)\\
&= \left(V_{\delta,i}(t) - V_{\delta,i-1}(t)\right) - \left(V_{\Xi,i}(t) - V_{\Xi,i-1}(t)\right)
\end{aligned} \tag{15}$$

where $\tilde{\boldsymbol{\Xi}}_i(t) = \boldsymbol{\Xi}(t) - \hat{\boldsymbol{\Xi}}_i(t)$ is the parameter estimation error.

Substituting control scheme (12) into (11), it yields

$$\begin{aligned} M\dot{\delta}_i(t) &= -\hat{\boldsymbol{\Xi}}_i^T(t)\boldsymbol{\xi}_i(t) + M\ddot{x}_r(t) - \alpha M\dot{e}_i(t) - \beta\delta_i(t) \\ &\quad + \boldsymbol{\Xi}_i^T(t)\boldsymbol{\xi}_i(t) - M\ddot{x}_r(t) + \alpha M\dot{e}_i(t) \\ &= \tilde{\boldsymbol{\Xi}}_i^T(t)\boldsymbol{\xi}_i(t) - \beta\delta_i(t) \end{aligned} \tag{16}$$

In terms of assumption 1, (15) and (16), there can be derived that

$$\begin{aligned} &V_{\delta,i}(t) - V_{\delta,i-1}(t) \\ &= \frac{1}{2}M\delta_i^2(t) - \frac{1}{2}M\delta_{i-1}^2(t) \\ &= \frac{1}{2}M\delta_i^2(0) + \int_0^t M\delta_i(\tau)\dot{\delta}_i(\tau)d\tau - \frac{1}{2}M\delta_{i-1}^2(t) \\ &= \int_0^t \delta_i(\tau)[\tilde{\boldsymbol{\Xi}}_i^T(\tau)\xi_i(\tau) - \beta\delta_i(\tau)]d\tau - \frac{1}{2}M\delta_{i-1}^2(t) \\ &= \int_0^t (\delta_i(\tau)\tilde{\boldsymbol{\Xi}}_i^T(\tau)\xi_i(\tau) - \beta\delta_i^2(\tau))d\tau - \frac{1}{2}M\delta_{i-1}^2(t) \end{aligned} \tag{17}$$

Using the parameter updating law (13), we have

$$\begin{aligned} &V_{\boldsymbol{\Xi},i}(t)) - V_{\boldsymbol{\Xi},i-1}(t) \\ &= \frac{1}{2}\int_0^t (\boldsymbol{\Xi}(\tau) - \hat{\boldsymbol{\Xi}}_i(\tau))^T\boldsymbol{\Gamma}^{-1}(\boldsymbol{\Xi}(\tau) - \hat{\boldsymbol{\Xi}}_i(\tau))d\tau \\ &\quad -\frac{1}{2}\int_0^t (\boldsymbol{\Xi}(\tau) - \hat{\boldsymbol{\Xi}}_{i-1}(\tau))^T\boldsymbol{\Gamma}^{-1}(\boldsymbol{\Xi}(\tau) - \hat{\boldsymbol{\Xi}}_{i-1}(\tau))d\tau \\ &= \frac{1}{2}\int_0^t 2(\boldsymbol{\Xi}(\tau) - \hat{\boldsymbol{\Xi}}_i(\tau))^T\boldsymbol{\Gamma}^{-1}(\hat{\boldsymbol{\Xi}}_{i-1}(\tau) - \hat{\boldsymbol{\Xi}}_i(\tau))d\tau \\ &\quad -\frac{1}{2}\int_0^t (\hat{\boldsymbol{\Xi}}_i(\tau) - \hat{\boldsymbol{\Xi}}_{i-1}(\tau))^T\boldsymbol{\Gamma}^{-1}(\hat{\boldsymbol{\Xi}}_i(\tau) - \hat{\boldsymbol{\Xi}}_{i-1}(\tau))d\tau \\ &= -\int_0^t \tilde{\boldsymbol{\Xi}}_i^T(\tau)\delta_i(\tau)\boldsymbol{\xi}_i(\tau)d\tau - \frac{1}{2}\int_0^t (\boldsymbol{\xi}_i(\tau))^T\boldsymbol{\Gamma}\boldsymbol{\xi}_i(\tau)\delta_i^2(\tau)d\tau \end{aligned} \tag{18}$$

Substituting (17) and (18) into (15), it can be derived that

$$\begin{aligned} &\Delta E_i(t) \\ &= E_i(t) - E_{i-1}(t) \\ &= \int_0^t (\delta_i(\tau)\tilde{\boldsymbol{\Xi}}_i^T(\tau)\boldsymbol{\xi}_i(t) - \beta\delta_i^2(\tau))d\tau - \frac{1}{2}M\delta_{i-1}^2(t) \\ &\quad -\int_0^t \tilde{\boldsymbol{\Xi}}_i^T(\tau)\delta_i(\tau)\boldsymbol{\xi}_i(\tau)d\tau - \frac{1}{2}\int_0^t (\boldsymbol{\xi}_i(\tau))^T\boldsymbol{\Gamma}\boldsymbol{\xi}_i(\tau)\delta_i^2(\tau)d\tau \\ &= \int_0^t -\beta\delta_i^2(\tau))d\tau - \frac{1}{2}\int_0^t (\boldsymbol{\xi}_i(\tau))^T\boldsymbol{\Gamma}\boldsymbol{\xi}_i(\tau)\delta_i^2(\tau)d\tau \\ &\quad -\frac{1}{2}M\delta_{i-1}^2(t) \\ &\leq -\frac{1}{2}M\delta_{i-1}^2(t) \end{aligned} \tag{19}$$

From (19), we can obtain $\Delta E_i(t) \leq 0$.

Part B: The boundness of $E_0(t)$

In terms of (19), for any iteration, since $E_0(t)$ is finite, it is clear that finiteness of $E_i(t)$. Hence, we will prove the finiteness of $E_0(t)$.

$$E_0(t) = \frac{1}{2}M\delta_0^2(t) + \frac{1}{2}\int_0^t \tilde{\boldsymbol{\Xi}}_0^T(\tau)\boldsymbol{\Gamma}^{-1}\tilde{\boldsymbol{\Xi}}_0(\tau)d\tau \tag{20}$$

At initial iteration, from (13), the parameter update law is

$$\begin{aligned} \hat{\boldsymbol{\Xi}}_0(t) &= \boldsymbol{\Gamma}\delta_0(t)\xi_0(t) \\ \delta_0(t)\xi_0(t) &= \boldsymbol{\Gamma}^{-1}\hat{\boldsymbol{\Xi}}_0(t) \end{aligned} \tag{21}$$

According to (12), (13) and (21), we have

$$\begin{aligned} \dot{E}_0(t) &= \frac{1}{2}M\delta_0^2(t) + \frac{1}{2}\int_0^t \tilde{\boldsymbol{\Xi}}_0^T(\tau)\boldsymbol{\Gamma}^{-1}\tilde{\boldsymbol{\Xi}}_0(\tau)d\tau \\ &= M\delta_0(t)\dot{\delta}_0(t) + \frac{1}{2}\tilde{\boldsymbol{\Xi}}_0^T(t)\boldsymbol{\Gamma}^{-1}\tilde{\boldsymbol{\Xi}}_0(t) \\ &= \delta_0(t)\tilde{\boldsymbol{\Xi}}_0^T(t)\boldsymbol{\xi}_0(t) - \beta\delta_0^2(t) + \frac{1}{2}\tilde{\boldsymbol{\Xi}}_0^T(t)\boldsymbol{\Gamma}^{-1}\tilde{\boldsymbol{\Xi}}_0(t) \\ &= \tilde{\boldsymbol{\Xi}}_0^T(t)\boldsymbol{\Gamma}^{-1}\hat{\boldsymbol{\Xi}}_0(t) - \beta\delta_0^2(t) + \frac{1}{2}\tilde{\boldsymbol{\Xi}}_0^T(t)\boldsymbol{\Gamma}^{-1}\tilde{\boldsymbol{\Xi}}_0(t) \\ &= \tilde{\boldsymbol{\Xi}}_0^T(t)\boldsymbol{\Gamma}^{-1}(\hat{\boldsymbol{\Xi}}_0(t) - \boldsymbol{\Xi}(t) + \boldsymbol{\Xi}(t)) - \beta\delta_0^2(t) \\ &\quad + \frac{1}{2}\tilde{\boldsymbol{\Xi}}_0^T(t)\boldsymbol{\Gamma}^{-1}\tilde{\boldsymbol{\Xi}}_0(t) \\ &= -\tilde{\boldsymbol{\Xi}}_0^T(t)\boldsymbol{\Gamma}^{-1}\tilde{\boldsymbol{\Xi}}_0(t) + \tilde{\boldsymbol{\Xi}}_0^T(t)\boldsymbol{\Gamma}^{-1}\boldsymbol{\Xi}(t) - \beta\delta_0^2(t) \\ &\quad + \frac{1}{2}\tilde{\boldsymbol{\Xi}}_0^T(t)\boldsymbol{\Gamma}^{-1}\tilde{\boldsymbol{\Xi}}_0(t) \\ &= -\frac{1}{2}\tilde{\boldsymbol{\Xi}}_0^T(t)\boldsymbol{\Gamma}^{-1}\tilde{\boldsymbol{\Xi}}_0(t) + \tilde{\boldsymbol{\Xi}}_0^T(t)\boldsymbol{\Gamma}^{-1}\boldsymbol{\Xi}(t) - \beta\delta_0^2(t) \end{aligned} \tag{22}$$

Using Young inequality, for any $0 < c < 1$, one has

$$\tilde{\boldsymbol{\Xi}}_0^T(t)\boldsymbol{\Gamma}^{-1}\boldsymbol{\Xi}(t) \leq c\tilde{\boldsymbol{\Xi}}_0^T(t)\boldsymbol{\Gamma}^{-1}\tilde{\boldsymbol{\Xi}}_0(t) + \frac{1}{4c}\boldsymbol{\Xi}^T(t)\boldsymbol{\Gamma}^{-1}\boldsymbol{\Xi}(t) \tag{23}$$

Further, choosing $c < 1/2$, it leads to

$$\begin{aligned} &\dot{E}_0(t) \\ &= -\frac{1}{2}\tilde{\boldsymbol{\Xi}}_0^T(t)\boldsymbol{\Gamma}^{-1}\tilde{\boldsymbol{\Xi}}_0(t) + \tilde{\boldsymbol{\Xi}}_0^T(t)\boldsymbol{\Gamma}^{-1}\boldsymbol{\Xi}(t) - \beta\delta_0^2(t) \\ &< -(\frac{1}{2} - c)c\tilde{\boldsymbol{\Xi}}_0^T(t)\boldsymbol{\Gamma}^{-1}\tilde{\boldsymbol{\Xi}}_0(t) - \beta\delta_0^2(t) + \frac{1}{4c}\boldsymbol{\Xi}^T(t)\boldsymbol{\Gamma}^{-1}\boldsymbol{\Xi}(t) \end{aligned} \tag{24}$$

Since $\boldsymbol{\Xi}(t)$ is the subway train system parameters vector which must be bounded, there must exist a uniform upper bound $\Xi_{\max}$ for these unknown parameters, such that $\boldsymbol{\Xi}(t) \leq \Xi_{\max}\mathbf{1}_3$, where $\mathbf{1}_3 = [1, 1, 1]^T$. In addition, $\tilde{\boldsymbol{\Xi}}_0(t)$ and $\delta_0(t)$ are all bounded.

Hence, $\dot{E}_0(t)$ is negative definite beyond the region

$$\left\{\delta_0 \in R, \tilde{\boldsymbol{\Xi}}_0 \in R^3 \middle| (\frac{1}{2} - c)c\tilde{\boldsymbol{\Xi}}_0^T(t)\boldsymbol{\Gamma}^{-1}\tilde{\boldsymbol{\Xi}}_0(t) + \beta\delta_0^2(t) \leq \frac{3\rho\Xi_{\max}^2}{4c}\right\}$$

which derives the boundness of $E_0(t)$ in the finite interval. ρ is the spectrum radius of matrix $\boldsymbol{\Gamma}^{-1}$.

Part C: The convergence of subway train tracking error

$$E_i(t) = E_0(t) + \sum_{j=1}^{i}\Delta E_j(t) \leq E_0(t) - \sum_{j=1}^{i}\frac{1}{2}M\delta_{j-1}^2(t) \tag{25}$$

$$\lim_{i\to\infty} E_i(t) \leq E_0(t) - \lim_{i\to\infty}\sum_{j=1}^{i}\frac{1}{2}M\delta_{j-1}^2(t) \tag{26}$$

Because $E_0(t)$ is bounded and $E_i(t)$ is positive, we have

$$\lim_{i\to\infty}\sum_{j=1}^{i}\frac{1}{2}M\delta_{j-1}^2(t) \leq E_0(t) \tag{27}$$

In terms of the convergence property of sum of series, there can be derived that

$$\lim_{i\to\infty} M\delta_i^2(t) = 0 \tag{28}$$

Hence, $\dot{e}_i(t) \to 0$ and $e_i(t) \to 0$ as $i \to \infty$.

Due to finiteness of $E_i(t)$, it can obtain that $\dot{e}_i(t)$ and $e_i(t)$ are limited. Since $x_r(t)$ and $\dot{x}_r(t)$ are bounded, it indicates that $x_i(t)$ and $\dot{x}_i(t)$ are limited, too. Furthermore, in terms of control law (12), $u_i(t)$ is also bounded.

IV. Speed Constraint Adaptive Iterative Learning Control

In order to avoid over speed, derailment and collision of the subway train, the problem of the speed constraint of the subway train must be considered for the control scheme design. In the automatic train control (ATC) system, the onboard ATP subsystem realizes the supervision of the subway train speed and over speed protection, which is important to ensure the safe operation of the subway train. The function of the onboard ATO subsystem is to conduct the speed control of the subway train under the constraints given by the onboard ATP subsystem. The speed protection curve, which is generated by automatic train protection, can be regarded as a kind of speed constraint $\nu_{\max}(t)$ for subway trains. Considering the safety and reliability of subway train operation, the subway train speed $\dot{x}_i(t)$ must satisfy $|\dot{x}_i(t)| < |\nu_{\max}(t)|$, $\forall t$. Obviously, the desired speed $\dot{x}_r(t)$ must satisfy $|\dot{x}_r(t)| \le |\nu_r(t)|$, where $|\nu_{\max}(t)| > |\nu_r(t)|$. $\upsilon_r(t)$ is the upper bound of desired speed $\dot{x}_r(t)$.

Firstly, to address the problem caused by the subway train speed constraint, a barrier Lyapunov function (BLF) is introduced as follows.

$$V_{b,i}(t) = \frac{\nu_b^2}{\pi}\tan\left(\frac{\pi\delta_i^2(t)}{2\nu_b^2}\right) \tag{29}$$

where $\nu_b > 0$ is a boundary parameter. If the augmented error $\delta_i(t)$ tends to ν_b, $V_{b,i}(t)$ will go to infinity. Hence, we design the adaptive iterative learning control law such that the BLF is bounded, which can ensure that the augmented error $\delta_i(t)$ is on the interval $(-\nu_b, \nu_b)$. Furthermore, the subway train speed cannot exceed the boundary speed $\nu_{\max}(t)$.

In the subway train operation control system, therefore, to ensure the safety and reliability, a speed constraint adaptive iterative learning control (CAILC) is proposed as

$$u_i(t) = -\hat{\boldsymbol{\Xi}}_i^T(t)\boldsymbol{\xi}_i(t) + M\ddot{x}_r(t) - M\alpha\dot{e}_i(t) - \beta\delta_i(t) \tag{30}$$

Considering the subway train speed constraint, the parameter updating law $\hat{\boldsymbol{\Xi}}_i(t)$ is designed as follows.

$$\hat{\boldsymbol{\Xi}}_i(t) = sat_{\Xi}[\bar{\boldsymbol{\Xi}}_i(t)] \tag{31}$$

$$\bar{\boldsymbol{\Xi}}_i(t) = \hat{\boldsymbol{\Xi}}_{i-1}(t) + \boldsymbol{\Gamma}\boldsymbol{\xi}_i(t)\chi_i(t),\ \hat{\boldsymbol{\Xi}}_{-1}(t) = 0 \tag{32}$$

where $\boldsymbol{\Gamma}$ is a positive definite adaptive diagonal matrix learning gain.

$$\chi_i(t) = \frac{dV_{b,i}(t)}{d\delta_i(t)} = \frac{\delta_i(t)}{\cos^2(\frac{\pi\delta_i^2(t)}{2\nu_b^2})} \tag{33}$$

The saturation function $sat_{\Xi}[\cdot]$ is given by

$$sat_{\Xi}[\bar{\Xi}_i(t)] = \{sat_{\Xi}[\bar{\phi}_{j,i}(t)]\},\quad j = 1,2,3 \tag{34}$$

$$sat_{\Xi}[\bar{\phi}_{j,i}] = \begin{cases} \phi_{j,\max} & \bar{\phi}_{j,i} > \phi_{j,\max} \\ \bar{\phi}_{j,i} & \phi_{j,\min} \le \bar{\phi}_{j,i} \le \phi_{j,\max} \\ \phi_{j,\min} & \bar{\phi}_{j,i} < \phi_{j,\min} \end{cases} \tag{35}$$

where $\phi_{j,\max}$ and $\phi_{j,\min}$ are the upper bound of the parameter estimation and the lower bound of parameter estimation, respectively. We assume that the subway train system parameters satisfy $\boldsymbol{\Xi}(t) \in [\boldsymbol{\Xi}_{\min}, \boldsymbol{\Xi}_{\max}]$, where $\boldsymbol{\Xi}_{\min} = \{\phi_{j,\min}\}$, $\boldsymbol{\Xi}_{\max} = \{\phi_{j,\max}\}$, $j = 1, 2, 3$.

For analysis convenience, Lemma1 is introduced.

Lemma 1: For any $\boldsymbol{\Xi}(t) \in [\boldsymbol{\Xi}_{\min}, \boldsymbol{\Xi}_{\max}]$, the following inequality is established [39].

$$[(\boldsymbol{\Xi}(t) - sat_{\Xi}[\bar{\boldsymbol{\Xi}}_i(t)])^T\boldsymbol{\Gamma}^{-1}(\bar{\boldsymbol{\Xi}}_i(t) - sat_{\Xi}[\bar{\boldsymbol{\Xi}}_i(t)])] \le 0 \tag{36}$$

Theorem 2: Considering the subway train system (9) satisfying assumption 1, the speed constraint adaptive iterative learning control (CAILC) laws (30)-(35) can ensure that the speed and position tracking error asymptotically converges to zero as the iteration number i goes to infinity, i.e. $\lim_{i\to\infty}\dot{e}_i(t) = 0$ and $\lim_{i\to\infty} e_i(t) = 0$. In addition, the speed constraint can be satisfied at any iteration.

Proof: The barrier composite energy function (BCEF) is designed as follows.

$$\begin{aligned} E_i(t) &= M\frac{\nu_b^2}{\pi}\tan\left(\frac{\pi\delta_i^2(t)}{2\nu_b^2}\right) + \frac{1}{2}\int_0^t \tilde{\boldsymbol{\Xi}}_i^T(\tau)\boldsymbol{\Gamma}^{-1}\tilde{\boldsymbol{\Xi}}_i(\tau)d\tau \\ &= V_{\delta,i}(t) + V_{\boldsymbol{\Xi},i}(t) \end{aligned} \tag{37}$$

where $V_{\delta,i}(t) = M\frac{\nu_b^2}{\pi}\tan\left(\frac{\pi\delta_i^2(t)}{2\nu_b^2}\right)$. $\tilde{\boldsymbol{\Xi}}_i(t) = \boldsymbol{\Xi}(t) - \hat{\boldsymbol{\Xi}}_i(t)$. $V_{\Xi,i}(t) = \int_0^t \tilde{\Xi}_i^T(\tau)\boldsymbol{\Gamma}^{-1}\tilde{\Xi}_i(\tau)d\tau/2$.

This proof includes four parts. *Part* A1 is to prove the non-increasing property of BCEF. *Part* B1 is the boundedness of $E_0(t)$. *Part* C1 is to show the tracking error convergence. Part D1 is the speed constraint.

Part A1: Non-increasing property of the BCEF

Considering the first term on the right hand side of BCEF (37), we note that

$$V_{\delta,i}(t) - V_{\delta,i-1}(t) = \frac{\nu_b^2}{\pi}\tan\left(\frac{\pi\delta_i^2(t)}{2\nu_b^2}\right) - \frac{\nu_b^2}{\pi}\tan\left(\frac{\pi\delta_{i-1}^2(t)}{2\nu_b^2}\right) \tag{38}$$

According to the subway train system error dynamic equation (16), parameter updating laws (31)-(35) and assumption 1, it can be derived that

$$\begin{aligned} V_{\delta,i}(t) &= M\frac{\nu_b^2}{\pi}\tan\left(\frac{\pi\delta_i^2(t)}{2\nu_b^2}\right) \\ &= \int_0^t \frac{\delta_i(\tau)M\dot{\delta}_i(\tau)}{\cos^2(\frac{\pi\delta_i^2(\tau)}{2\nu_b^2})}d\tau + M\frac{\nu_b^2}{\pi}\tan\left(\frac{\pi\delta_i^2(0)}{2\nu_b^2}\right) \\ &= \int_0^t (\chi_i(\tau)\tilde{\boldsymbol{\Xi}}_i^T(\tau)\boldsymbol{\xi}_i(\tau) - \chi_i(\tau)\beta\delta_i(\tau))d\tau \end{aligned} \tag{39}$$

which further implies that

$$\begin{aligned} & V_{\delta,i}(t) - V_{\delta,i-1}(t) \\ & = \int_0^t (\chi_i(\tau)\tilde{\boldsymbol{\Xi}}_i^T(\tau)\boldsymbol{\xi}_i(\tau) - \chi_i(\tau)\beta\delta_i(\tau))d\tau \\ & \quad -M\frac{v_b^2}{\pi}\tan\left(\frac{\pi\delta_{i-1}^2(t)}{2v_b^2}\right) \end{aligned} \tag{40}$$

From the second term on the right hand side of BCEF (37), we can obtain

$$\begin{aligned} & V_{\Xi,i}(t) - V_{\Xi,i-1}(t) \\ & = \frac{1}{2}\int_0^t \tilde{\Xi}_i^T(\tau)\boldsymbol{\Gamma}^{-1}\tilde{\Xi}_i(\tau)d\tau - \frac{1}{2}\int_0^t \tilde{\Xi}_{i-1}^T(\tau)\boldsymbol{\Gamma}^{-1}\tilde{\Xi}_{i-1}(\tau)d\tau \\ & = \frac{1}{2}\int_0^t (\Xi(\tau) - \hat{\Xi}_i(\tau))^T\boldsymbol{\Gamma}^{-1}(\Xi(\tau) - \hat{\Xi}_i(\tau))d\tau \\ & \quad -\frac{1}{2}\int_0^t (\Xi(\tau) - \hat{\Xi}_{i-1}(\tau))^T\boldsymbol{\Gamma}^{-1}(\Xi(\tau) - \hat{\Xi}_{i-1}(\tau))d\tau \\ & = \frac{1}{2}\int_0^t 2(\Xi(\tau) - \hat{\Xi}_i(\tau))^T\boldsymbol{\Gamma}^{-1}(\hat{\Xi}_{i-1}(\tau) - \hat{\Xi}_i(\tau)) \\ & \quad -(\hat{\Xi}_i(\tau) - \hat{\Xi}_{i-1}(\tau))^T\boldsymbol{\Gamma}^{-1}(\hat{\Xi}_i(\tau) - \hat{\Xi}_{i-1}(\tau))d\tau \\ & = \int_0^t (\Xi(\tau) - \hat{\Xi}_i(\tau))^T\boldsymbol{\Gamma}^{-1}(\hat{\Xi}_{i-1}(\tau) - \hat{\Xi}_i(\tau))d\tau \\ & \quad -\frac{1}{2}\int_0^t (\hat{\Xi}_i(\tau) - \hat{\Xi}_{i-1}(\tau))^T\boldsymbol{\Gamma}^{-1}(\hat{\Xi}_i(\tau) - \hat{\Xi}_{i-1}(\tau))d\tau \end{aligned} \tag{41}$$

Using lemma 1, parameter updating laws (31)-(35) and (41), it comes

$$\begin{aligned} & V_{\boldsymbol{\Xi},i}(t) - V_{\boldsymbol{\Xi},i-1}(t) \\ & = \int_0^t (\boldsymbol{\Xi}(\tau) - sat_{\boldsymbol{\Xi}}[\bar{\boldsymbol{\Xi}}_i(\tau)])^T\boldsymbol{\Gamma}^{-1}(\bar{\boldsymbol{\Xi}}_i(\tau) - \boldsymbol{\Gamma}\boldsymbol{\xi}_i(\tau)\chi_i(\tau) \\ & \quad -sat_{\boldsymbol{\Xi}}[\bar{\boldsymbol{\Xi}}_i(\tau)])d\tau \\ & \quad -\frac{1}{2}\int_0^t (\hat{\boldsymbol{\Xi}}_i(\tau) - \hat{\boldsymbol{\Xi}}_{i-1}(\tau))^T\boldsymbol{\Gamma}^{-1}(\hat{\boldsymbol{\Xi}}_i(\tau) - \hat{\boldsymbol{\Xi}}_{i-1}(\tau))d\tau \\ & = -\int_0^t (\boldsymbol{\Xi}(\tau) - sat_{\boldsymbol{\Xi}}[\bar{\boldsymbol{\Xi}}_i(\tau)])^T\boldsymbol{\Gamma}^{-1}(sat_{\boldsymbol{\Xi}}[\bar{\boldsymbol{\Xi}}_i(\tau)] - \bar{\boldsymbol{\Xi}}_i(\tau))d\tau \\ & \quad -\int_0^t (\boldsymbol{\Xi}(\tau) - \hat{\boldsymbol{\Xi}}_i(\tau))^T\boldsymbol{\xi}_i(\tau)\chi_i(\tau)d\tau \\ & \quad -\frac{1}{2}\int_0^t (\hat{\boldsymbol{\Xi}}_i(\tau) - \hat{\boldsymbol{\Xi}}_{i-1}(\tau))^T\boldsymbol{\Gamma}^{-1}(\hat{\boldsymbol{\Xi}}_i(\tau) - \hat{\boldsymbol{\Xi}}_{i-1}(\tau))d\tau \\ & \le -\int_0^t \tilde{\boldsymbol{\Xi}}_i(\tau)^T\boldsymbol{\xi}_i(t)\chi_i(\tau)d\tau \\ & \quad -\frac{1}{2}\int_0^t (\hat{\boldsymbol{\Xi}}_i(\tau) - \hat{\boldsymbol{\Xi}}_{i-1}(\tau))^T\boldsymbol{\Gamma}^{-1}(\hat{\boldsymbol{\Xi}}_i(\tau) - \hat{\boldsymbol{\Xi}}_{i-1}(\tau))d\tau \end{aligned} \tag{42}$$

Therefore, in terms of (40) and (42), we can deduce that

$$\begin{aligned} & \Delta E_i(t) \\ & = E_i(t) - E_{i-1}(t) \\ & \le \int_0^t (\chi_i(\tau)\tilde{\boldsymbol{\Xi}}_i^T(\tau)\boldsymbol{\xi}_i(\tau) - \chi_i(\tau)\beta\delta_i(\tau))d\tau \\ & \quad -M\frac{v_b^2}{\pi}\tan\left(\frac{\pi\delta_{i-1}^2(t)}{2v_b^2}\right) - \int_0^t \tilde{\boldsymbol{\Xi}}_i(\tau)^T\boldsymbol{\xi}_i(\tau)\chi_i(\tau)d\tau \\ & \quad -\frac{1}{2}\int_0^t (\hat{\boldsymbol{\Xi}}_i(\tau) - \hat{\boldsymbol{\Xi}}_{i-1}(\tau))^T\boldsymbol{\Gamma}^{-1}(\hat{\boldsymbol{\Xi}}_i(\tau) - \hat{\boldsymbol{\Xi}}_{i-1}(\tau))d\tau \\ & = -\int_0^t \chi_i(\tau)\beta\delta_i(\tau))d\tau - M\frac{v_b^2}{\pi}\tan\left(\frac{\pi\delta_{i-1}^2(t)}{2v_b^2}\right) \\ & \quad -\frac{1}{2}\int_0^t (\hat{\boldsymbol{\Xi}}_i(\tau) - \hat{\boldsymbol{\Xi}}_{i-1}(\tau))^T\boldsymbol{\Gamma}^{-1}(\hat{\boldsymbol{\Xi}}_i(\tau) - \hat{\boldsymbol{\Xi}}_{i-1}(\tau))d\tau \end{aligned} \tag{43}$$

Since $\chi_i(t) = \frac{\delta_i(t)}{\cos^2(\frac{\pi\delta_i^2(t)}{2v_b^2})}$, and $\chi_i(t)\beta\delta_i(t) \ge 0$, we have

$$\Delta E_i(t) \le -M\frac{v_b^2}{\pi}\tan\left(\frac{\pi\delta_{i-1}^2(t)}{2v_b^2}\right) \le 0 \tag{44}$$

From (44), it can be seen that the BCEF is decreasing in the iterative axis.

Part B1: Boundedness of $E_0(t)$.

According to (37), we obtain

$$E_0(t) = M\frac{v_b^2}{\pi}\tan\left(\frac{\pi\delta_0^2(t)}{2v_b^2}\right) + \frac{1}{2}\int_0^t \tilde{\boldsymbol{\Xi}}_0^T(\tau)\boldsymbol{\Gamma}^{-1}\tilde{\boldsymbol{\Xi}}_0(\tau)d\tau \tag{45}$$

By virtue of parameter updating laws (32) and (33), it leads to

$$\begin{aligned} \bar{\boldsymbol{\Xi}}_0(t) &= \hat{\boldsymbol{\Xi}}_{-1}(t) + \boldsymbol{\Gamma}\boldsymbol{\xi}_0(t)\chi_0(t) = \boldsymbol{\Gamma}\boldsymbol{\xi}_0(t)\chi_0(t) \\ \boldsymbol{\xi}_0(t)\chi_0(t) &= \boldsymbol{\Gamma}^{-1}\bar{\boldsymbol{\Xi}}_0(t) \end{aligned} \tag{46}$$

Using lemma 1, combining with (45) and (46) results in

$$\begin{aligned} \dot{E}_0(t) &= \frac{\delta_0(t)M\dot{\delta}_0(t)}{\cos^2(\frac{\pi\delta_0^2(t)}{2v_b^2})} + \frac{1}{2}\tilde{\boldsymbol{\Xi}}_0^T(t)\boldsymbol{\Gamma}^{-1}\tilde{\boldsymbol{\Xi}}_0(t) \\ &= \chi_0(t)\tilde{\boldsymbol{\Xi}}_0^T(t)\boldsymbol{\xi}_0(t) - \chi_0(t)\beta\delta_0(t) + \frac{1}{2}\tilde{\boldsymbol{\Xi}}_0^T(t)\boldsymbol{\Gamma}^{-1}\tilde{\boldsymbol{\Xi}}_0(t) \\ &\le \tilde{\boldsymbol{\Xi}}_0^T(t)\boldsymbol{\Gamma}^{-1}\bar{\boldsymbol{\Xi}}_0(t) + \tilde{\boldsymbol{\Xi}}_0^T(t)\boldsymbol{\Gamma}^{-1}\tilde{\boldsymbol{\Xi}}_0(t) - \chi_0(t)\beta\delta_0(t) \\ &= \tilde{\boldsymbol{\Xi}}_0^T(t)\boldsymbol{\Gamma}^{-1}\bar{\boldsymbol{\Xi}}_0(t) + \tilde{\boldsymbol{\Xi}}_0^T(t)\boldsymbol{\Gamma}^{-1}\left(\boldsymbol{\Xi}(t) - \hat{\boldsymbol{\Xi}}_0(t)\right) \\ &\quad -\chi_0(t)\beta\delta_0(t) \\ &= \left(\boldsymbol{\Xi}(t) - sat_{\Xi}[\bar{\boldsymbol{\Xi}}_0(t)]\right)^T\boldsymbol{\Gamma}^{-1}\left(\bar{\boldsymbol{\Xi}}_0(t) - sat_{\Xi}[\bar{\boldsymbol{\Xi}}_0(t)]\right) \\ &\quad +\tilde{\boldsymbol{\Xi}}_0^T(t)\boldsymbol{\Gamma}^{-1}\boldsymbol{\Xi}(t) - \chi_0(t)\beta\delta_0(t) \\ &\le \tilde{\boldsymbol{\Xi}}_0^T(t)\boldsymbol{\Gamma}^{-1}\boldsymbol{\Xi}(t) - \chi_0(t)\beta\delta_0(t) \end{aligned} \tag{47}$$

$\boldsymbol{\Gamma}^{-1}$ stands for the positive definite diagonal matrix. Utilizing the Young inequality, $0 < c < 1$, one has

$$\tilde{\boldsymbol{\Xi}}_0^T(t)\boldsymbol{\Gamma}^{-1}\boldsymbol{\Xi}(t) \le c\tilde{\boldsymbol{\Xi}}_0^T(t)\boldsymbol{\Gamma}^{-1}\tilde{\boldsymbol{\Xi}}_0(t) + \frac{1}{4c}\boldsymbol{\Xi}^T(t)\boldsymbol{\Gamma}^{-1}\boldsymbol{\Xi}(t) \tag{48}$$

It can be obtain

$$\begin{aligned} \dot{E}_0(t) &\le \tilde{\boldsymbol{\Xi}}_0^T(t)\boldsymbol{\Gamma}^{-1}\boldsymbol{\Xi}(t) - \chi_0(t)\beta\delta_0(t) \\ &\le c\tilde{\boldsymbol{\Xi}}_0^T(t)\boldsymbol{\Gamma}^{-1}\tilde{\boldsymbol{\Xi}}_0(t) + \frac{1}{4c}\boldsymbol{\Xi}^T(t)\boldsymbol{\Gamma}^{-1}\boldsymbol{\Xi}(t) - \chi_0(t)\beta\delta_0(t) \end{aligned} \tag{49}$$

Since $\boldsymbol{\Xi}(t)$ is a bounded parameters vector of the subway train system, there must exist a uniform upper bound $\Xi_{\max}$ for these unknown parameters, such that $\boldsymbol{\Xi}(t) \le \Xi_{\max}\mathbf{1}_3$, where $\mathbf{1}_3 = [1, 1, 1]^T$. According to (31)-(36), $\tilde{\boldsymbol{\Xi}}_0(t)$, $\delta_0(t)$ and $\chi_0(t)$ are all bounded.

Therefore, $\dot{E}_0(t)$ is negative definite outside the region

$$\left\{\delta_0 \in R, \tilde{\boldsymbol{\Xi}}_0 \in R^3 \,\middle|\, -c\tilde{\boldsymbol{\Xi}}_0^T(t)\boldsymbol{\Gamma}^{-1}\tilde{\boldsymbol{\Xi}}_0(t) + \chi_0(t)\beta\delta_0(t) \le \frac{3\rho\Xi_{\max}^2}{4c}\right\}.$$

It can be derived the boundness of $E_0(t)$ in the finite interval. ρ is spectrum radius of matrix $\boldsymbol{\Gamma}^{-1}$.

Part C1: The convergence of tracking error

$$
\begin{aligned}
E_i(t) &= E_0(t) + \sum_{j=1}^{i} \Delta E_j(t) \\
&\leq E_0(t) - \sum_{j=1}^{i} M \frac{v_b^2}{\pi} \tan\left(\frac{\pi \delta_{j-1}^2(t)}{2v_b^2}\right) \\
\lim_{i\to\infty} E_i(t) &\leq E_0(t) - \lim_{i\to\infty} \sum_{j=1}^{i} M \frac{v_b^2}{\pi} \tan\left(\frac{\pi \delta_{j-1}^2(t)}{2v_b^2}\right)
\end{aligned}
$$

Because $E_0(t)$ is bounded, and $E_i(t)$ is positive, one has

$$\lim_{i\to\infty} \sum_{j=1}^{i} M \frac{v_b^2}{\pi} \tan\left(\frac{\pi \delta_{j-1}^2(t)}{2v_b^2}\right) \leq E_0(t) \tag{50}$$

In terms of the convergence property of the sum of series, we can deduce that

$$\lim_{i\to\infty} M \frac{v_b^2}{\pi} \tan\left(\frac{\pi \delta_{i-1}^2(t)}{2v_b^2}\right) = 0 \tag{51}$$

Therefore, we have $\lim_{i\to\infty} \delta_i(t) = 0$, $\lim_{i\to\infty} \dot{e}_i(t) = 0$ and $\lim_{i\to\infty} e_i(t) = 0$.

Part D1: Speed constraint

Because $\tilde{\boldsymbol{\Xi}}_i(t)$ and $E_i(t)$ are finite, the BCEF $V_{b,i}(t) = \frac{v_b^2}{\pi} \tan\left(\frac{\pi \delta_i^2(t)}{2v_b^2}\right)$ is bounded. $|\delta_i(t)| < v_b$ is held. Since $\delta_i(t) = \alpha e_i(t) + \dot{e}_i(t)$, there must exist a bound function $v_{\dot{e}}(t)$ satisfying $0 < |v_{\dot{e}}(t)| < v_b$, such that $|\dot{e}_i(t)| < |v_{\dot{e}}(t)|$. Since $\dot{e}_i(t) = \dot{x}_i(t) - \dot{x}_r(t)$, $|\dot{x}_r(t)| \leq |v_r(t)|$, $|\dot{x}_i(t)| < |v_{\max}(t)|$ and $|v_{\max}(t)| > |v_r(t)|$, one can choose a proper v_b such that $0 < |v_{\dot{e}}(t)| \leq v_b < |v_{\max}(t)| - |v_r(t)|$. Since $|\dot{x}_i(t)| \leq |\dot{e}_i(t)| + |\dot{x}_r(t)|$, it can be obtained $|\dot{x}_i(t)| \leq |\dot{e}_i(t)| + |\dot{x}_r(t)| < |v_{\dot{e}}(t)| + |v_r(t)| < v_b + |v_r(t)| < |v_{\max}(t)|$, for any t. The boundedness of $\dot{e}_i(t)$ and $\dot{x}_r(t)$ implies that the speed $\dot{x}_i(t)$ is limit by predefined constraint.

V. Optimal Traction/Braking Distribution

The subway train is generally distributed driving type, which consists of several motoring vehicles and trailers. After subway train traction/braking force $u_i(t)$ is designed, we will conduct optimal distribution of the subway train traction/braking force $u_i(t)$ for each vehicle. If the vehicle is a motoring vehicle, it can provide traction $F_p(t)$ and braking forces $F_b(t)$. If the vehicle is a trailer, it merely offers braking force during the braking phase. To deal with the subway train traction/braking force $u_i(t)$ optimal distribution, the optimal criterion is given as [35].

$$
\begin{aligned}
&\min_{F_i} J(\boldsymbol{F}_i(t)) = \frac{1}{2} F_i^T(t) \boldsymbol{Q} \boldsymbol{F}_i(t) \\
&\text{s.t.} \boldsymbol{\Upsilon} \boldsymbol{F}_i(t) = u_i(t)
\end{aligned} \tag{52}
$$

where $\boldsymbol{F}_i(t) = [F_i^{(1)}(t), F_i^{(2)}(t), \cdots, F_i^{(n)}(t)]^T$ is the traction/braking force. $\boldsymbol{Q}$ denotes a positive definite matrix which can be selected by designer.

Using the lagrangian technique and (52), we have

$$\boldsymbol{F}_i(t) = \boldsymbol{Q}^{-1} \boldsymbol{\Upsilon}^T [\boldsymbol{\Upsilon} Q^{-1} \boldsymbol{\Upsilon}^T]^{-1} u_i(t) \tag{53}$$

If $u_i > 0$, only motoring vehicle can provide traction force. If $u_i < 0$, the motoring vehicle and trailer all offer braking forces for the subway train.

A subway train includes n vehicles with w motoring vehicles and q trailers. Considering w motoring vehicles, one has

$$
\begin{aligned}
&F_{pi}^{(k)}(t) = \lambda F_i^{(k)}(t), k \in \{M_c \,|M_c = 1, 2, \cdots, w\} \\
&F_{bi}^{(k)}(t) = \rho F_i^{(k)}(t)
\end{aligned} \tag{54}
$$

where $F_{pi}^{(k)}(t)$ and $F_{bi}^{(k)}(t)$ are traction and braking force for the k-th vehicle at i-th iteration.

For q trailers, we also have

$$F_{bi}^{(j)}(t) = \rho F_i^{(j)}(t), j \in \{T \,|T = 1, 2, \cdots, q\} \tag{55}$$

$$\lambda = \begin{cases} 1 & \text{if } \operatorname{sign}(u_i) > 0 \\ 0 & \text{if } \operatorname{sign}(u_i) < 0 \end{cases}, \quad \rho = \begin{cases} 0 & \text{if } \operatorname{sign}(u_i) > 0 \\ 1 & \text{if } \operatorname{sign}(u_i) < 0 \end{cases} \tag{56}$$

where the set M_c denotes motoring vehicles; the set T denotes trailers.

Remark 4: The passenger comfort is the problem of the impact of acceleration and deceleration generated by subway train operation on passengers. When acceleration and deceleration are smooth, it can be considered comfortable. The proposed AILC method can guarantee the perfect tracking of the actual subway train position-speed profile to the desired profile which is pre-designed by large number of experiments considering comprehensively the safety, comfort, energy, etc. of a subway train, and the speed constraint is satisfied at all iteration.

Remark 5: As the increase of the subway train speed, the high safety and reliable operation requirements for subway trains are must be satisfied. The large number of safety accidents has shown that the overspeed and the deviation to the desired position-speed profile are the vital factors. Over speed can cause derailment and collision of the subway train, so that the speed constraint is an important issue to ensure the safe and reliable operation of the subway train. Therefore, the speed constraint based control method can meet the speed limit requirement to guarantee the subway train running more safely and reliably.

Remark 6: In practice, some suggestions on implementation are as follows. Firstly, the proposed subway train control algorithms (30)-(35) are written to the onboard ATO controller. Secondly, the collected speed and position information of the subway train are transmitted to the onboard ATO controller through the cable, and then compared with the desired speed and position trajectory. The proposed control algorithms (30)-(35) are based on the speed error information, the position error information, the desired acceleration information, and the subway train parameters estimation information to calculate train control commands. In addition, a memory is needed to store the parameter information of the previous subway train operation, which is used to update the parameters of the current subway train operation. Finally, through the interface with the vehicle system, the onboard ATO equipment issues traction and braking commands to control the subway train to run and stop between stations, and start operations. With the increase of train running times, the control performance will be improved by using the proposed control method.

VI. Simulation

To show the effectiveness of the proposed control algorithms, two simulation examples of the subway train are conducted. The subway train is distributed driving type including three motoring vehicles with traction/braking capabilities, and three trailers with braking capabilities [40]. In this section, it is specified that $k = \{2, 4, 5\}$ is the number of motoring vehicles and $k = \{1, 3, 6\}$ stands for the number of trailers.

A. Example 1 (Without Disturbances)

The basic resistance coefficients for each vehicle are as follows [12], [41]. The basic resistance coefficients of motoring vehicles are given by

$$\begin{aligned} a^{(k)}(t) &= 0.275 \times \sin(0.0039t) + 1.2799, k = \{2, 4, 5\} \\ b^{(k)}(t) &= 0.0024 \times \sin(0.0039t) + 0.02517 \\ c^{(k)}(t) &= 4.65 \times 10^{-5} \times \sin(0.0039t) + 2.995 \times 10^{-4} \end{aligned} \tag{57}$$

The basic resistance coefficients of trailers are

$$\begin{aligned} a^{(k)}(t) &= 0.275 \times \sin(0.002t) + 1.28, k = \{1, 3, 6\} \\ b^{(k)}(t) &= 0.0024 \times \sin(0.002t) + 0.0252 \\ c^{(k)}(t) &= 4.65 \times 10^{-5} \times \sin(0.002t) + 2.996 \times 10^{-4} \end{aligned} \tag{58}$$

The spring deformations of the coupler varies are designed as follows

$$\begin{aligned} s^{(k)}(t) &= 0.1 \sin(t) \times 10^{-3}(\text{m}), \quad k = 1, 3, 6 \\ s^{(k)}(t) &= 0.15 \cos(t) \times 10^{-3}(\text{m}), \quad k = 2, 4, 5 \end{aligned} \tag{59}$$

The travel distance of a subway train for the simulation is 3512m including five cruise phases and three braking phases. The travel time is 190s. The maximum speed of the subway train is 80km/h [42], which is shown in Fig. 3. $t \in [0, 190]$. The masses of each vehicle are given as $m^{(1)} = 32.939 \times 10^3$(kg), $m^{(2)} = 32.957 \times 10^3$(kg), $m^{(3)} = 27.09 \times 10^3$(kg), $m^{(4)} = 34.05 \times 10^3$(kg), $m^{(5)} = 33.785 \times 10^3$(kg), $m^{(6)} = 33.474 \times 10^3$(kg) [40]. When maximum speed is 80km/h, the maximum acceleration and the maximum deceleration do not exceed 1.5 m/s^2. The initial values of the subway train are $u_i(0) = 0$, $x_i(0) = 0$, $\dot{x}_i(0) = 0$. $\boldsymbol{\Upsilon} = [1, 0.5, 0.4, 0.6, 1, 0.5]$.

Fig. 2 plots the unit additional resistance profile including the tunnel resistance, the curve resistance because of railway curvature and the gradient resistance due to the slope.

To verify the effectiveness and advantage of the proposed control method, the traditional PD type iterative learning control (PDILC) and adaptive control are given for comparison. Hence, there are three control schemes are applied to the subway train system in the simulation.

In the initial iteration, we adopt the following PID controller to generate the input and output data for CAILC and PDILC.

$$u(t) = \gamma_P \varepsilon(t) + \gamma_I \int_0^t \varepsilon(\tau) d\tau + \gamma_D \dot{\varepsilon}(t) \tag{60}$$

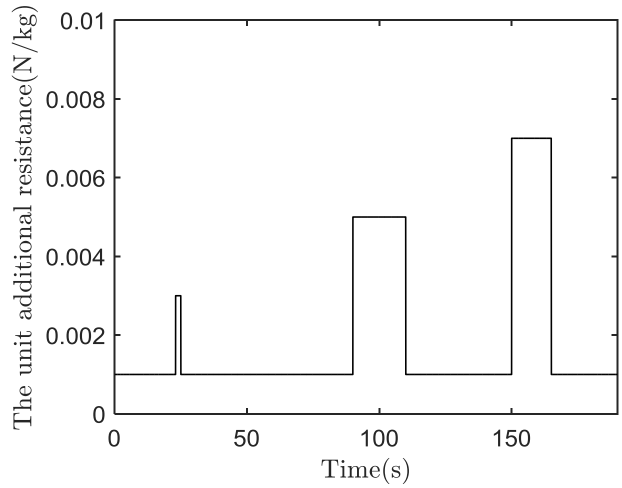

Fig. 2. The unit additional resistance.

where $\varepsilon(t) = \dot{x}_r(t) - \dot{x}_i(t)$ is speed tracking error of the subway train. γ_P, γ_I and γ_D are feedback gains, which are selected as $\gamma_p = 300201$, $\gamma_I = 1$, $\gamma_D = 10$.

Control scheme 1: The proposed speed constraint adaptive iterative learning control (CAILC) algorithms (30)-(35) are used for the subway train control system. The following parameters for CAILC algorithms are utilized. $\nu_b = 0.1$, $\alpha = 8$, $\beta = 1.1 \times 10^5$, $\boldsymbol{\Gamma} = diag\{100, 0.01, 0.01\}$, $\boldsymbol{\Xi}_{\max} = [1139.1, 0.0161, 0.002]^T$, $\boldsymbol{\Xi}_{\min} = [1120.3, 0.15, 0.0015]^T$, $\boldsymbol{Q} = diag\{0.1, 0.1, 0.1, 0.1, 0.1, 0.1\}$.

Control scheme 2: The PDILC [43] is applied.

$$u_i(t) = u_{i-1}(t) + k_p \varepsilon_i(t) + k_D \dot{\varepsilon}_i(t) \tag{61}$$

where $k_p = 1.05 \times 10^5$, $k_D = 1$.

Control scheme 3: Adaptive control in [35] is

$$u_i(t) = -(g_0 + \frac{\hat{\hbar} \bar{\lambda}^2(t)}{\bar{\lambda}(t) |\delta_i(t)| + \varepsilon_1}) \delta_i(t) \tag{62}$$

$$\dot{\hat{\hbar}} = -g_1 \hat{\hbar} + g_2 \frac{\bar{\lambda}^2(t) |\delta_i(t)|^2}{\bar{\lambda}(t) |\delta_i(t)| + \varepsilon_1} \tag{63}$$

where $g_0 > 0$, $g_1 > 0$, $g_2 > 0$, $\varepsilon_1 > 0$. $\bar{\lambda}(t) = 1 + |\dot{x}(t)| + |\dot{x}(t)|^2$.

Speed limit $v_{\max}(t)$ relies on the characteristics of the subway train and the line conditions, which is usually a piecewise constant function [4], [7], [44]. Speed limit $v_{\max}(t)$ is defined as follows

$$v_{\max}(t) = \begin{cases} 19.6(\text{m/s}), & t \in [0, 25] \\ 22.6(\text{m/s}), & t \in (25, 100] \\ 19.6(\text{m/s}), & t \in (100, 110] \\ 22.6(\text{m/s}), & t \in (110, 160] \\ 19.6(\text{m/s}), & t \in (160, 190] \end{cases} \tag{64}$$

Fig. 3 plots the speed tracking performance of subway train system by using the proposed CAILC, PDILC and adaptive control at the first iteration along the time axis. From Fig. 3, using PDILC method, it is clear that the speed exceeds the speed limit at some time at the first iteration. It is unsafe for subway train operation, since over speed can cause derailment

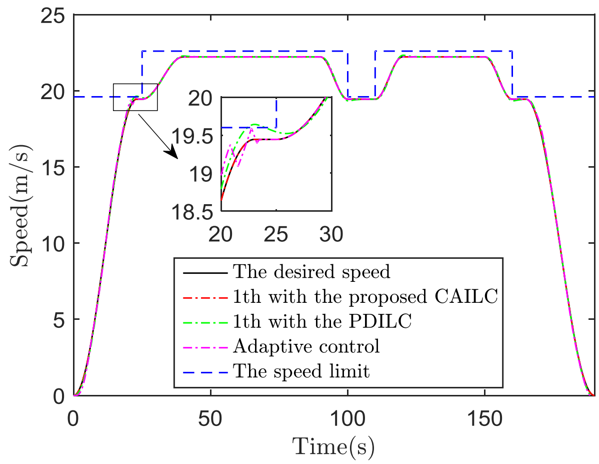

Fig. 3. Speed tracking profile with the proposed CAILC, PDILC and adaptive control at the 1th iteration.

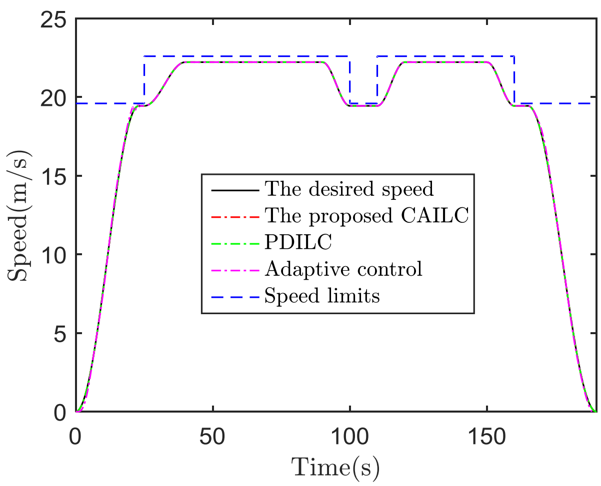

Fig. 4. Speed tracking profile with the proposed CAILC, PDILC and adaptive control at the 10th iteration.

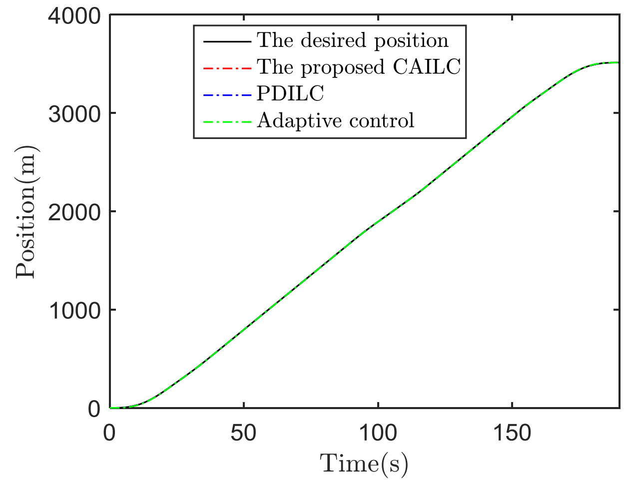

Fig. 5. Position tracking profile with the proposed CAILC, PDILC and adaptive control at the 10th iteration.

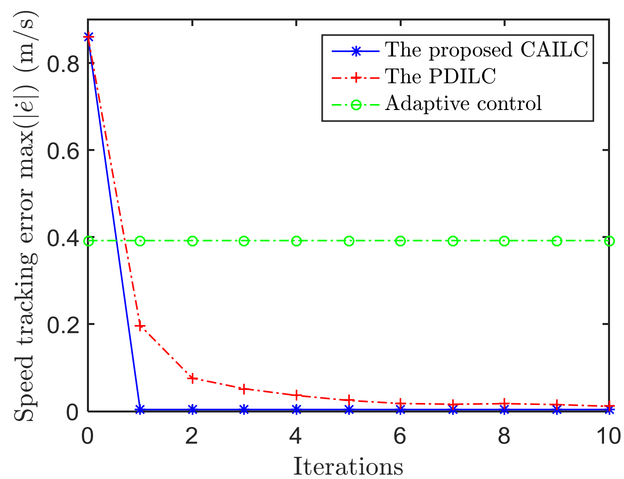

Fig. 6. The maximum speed tracking error with the proposed CAILC, PDILC and adaptive control.

and collision of the subway train. While, considering the speed constraint, the subway train speed is limited within the speed protection curve with the proposed CAILC in any iteration. Using the adaptive control method, there appears bad tracking performance. Compared with PDILC and adaptive control, the proposed CAILC has better control performance.

Fig. 4 and Fig. 5 are the speed and position tracking profiles at the $10th$ iteration along the time axis, respectively, where the dotted line represents the train output trajectory and the solid line denotes the desired trajectory. After 10 iterations, the desired speed and position can be tracked perfectly by using the proposed control algorithm. Fig. 6 and Fig. 7 plot the maximum speed tracking error profile and the maximum position tracking error profile in the iteration axis, which indicates that the presented CAILC possesses better convergent performance than PDILC and adaptive control. Since parameters updating laws of CAILC contains barrier Lyapunov function, which can improve control performance. In addition, because the adaptive control is a feedback control strategy in time domain, the control performance for the subway train cannot be improved as the times of the subway train operation increase. From Fig. 6 and Fig. 7, it is indicates that with the proposed CAILC, e_i and $\dot{e}_i(t)$ asymptotically converge to zero, as $i \to \infty$.

Meanwhile, to ensure the safety of subway train operation and passenger comfort, during the operation of a subway train, the acceleration and deceleration are smooth and the maximum acceleration and the maximum deceleration of a subway train are no more than $1.5m/s^2$ under the maximum speed 80 km/h [45]. Fig. 8 shows the acceleration and deceleration profile with the proposed CAILC, which is no more than $1.5m/s^2$. Using the adaptive control method, there appears jitter phenomenon, which will affect the comfort of passengers.

Using the proposed CAILC, the maximum augmented error is 0.0667, the maximum speed tracking error is 0.00388, and the maximum position tracking error is 0.00834 in all iteration. In the simulation, we select $\nu_b = 0.1$. According to *Theorem*2, it shows that $|\delta_i(t)| < \nu_b$ and $0 \leq |\dot{e}_i(t)| \leq \nu_b$. It can be derived that $|\dot{x}_i(t)| \leq |\dot{e}_i(t)| + |\dot{x}_r(t)| < \nu_b + |\nu_r(t)| < |\nu_{\max}(t)|, \forall t$. The speed constraint adaptive iterative learning control (CAILC) can guarantee that the augmented

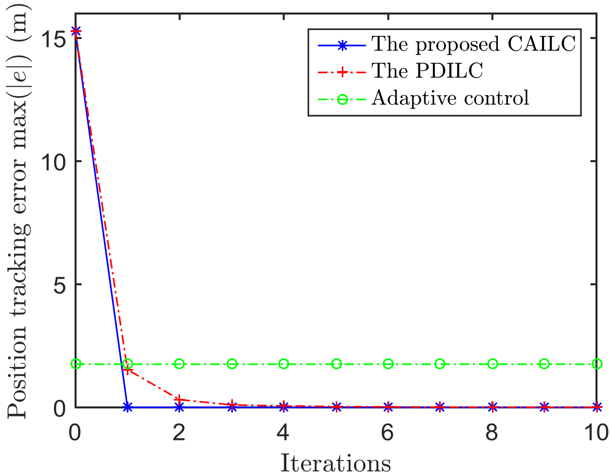

Fig. 7. The maximum position tracking error with the proposed CAILC, PDILC and adaptive control.

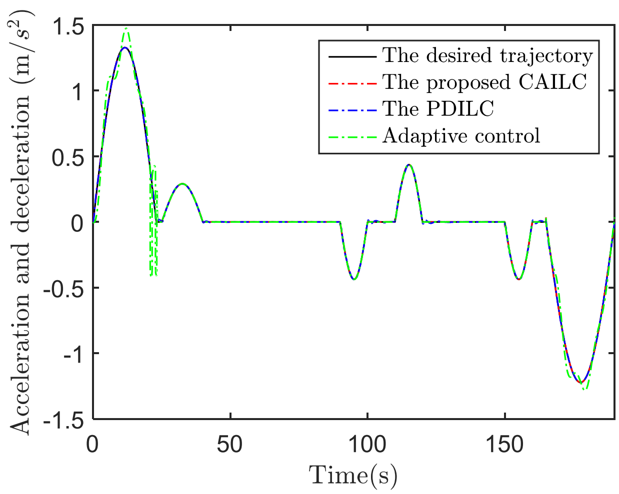

Fig. 8. Acceleration and deceleration profile with the proposed CAILC, PDILC and adaptive control.

error and speed tracking error do not exceed the bound v_b, which satisfies safety and reliable operation requirements of the subway train.

Fig. 9 and Fig. 10 show the control traction/braking forces contributed by each vehicle of the subway train. From Fig. 9 and Fig. 10, it indicates that in the traction and braking phase, the motoring vehicles offer both the traction forces and the braking forces. The trailers only offer the braking forces during the braking phase.

From the simulation results, it is known that the presented subway train control method can ensure the safe and reliable operation of the subway train. The simulation results verify advantages and effectiveness of our theoretical studies.

B. Example 2 (Simulation Analysis of Robustness)

In the process of subway train operation, it is inevitable to be affected by various disturbances, such as unknown load disturbance, measurement noise and the impact of a gust of wind. These disturbances will affect the performance of train tracking control. In order to verify the robustness of the proposed algorithm, this section studies simulation of the subway train operation tracking control under disturbance.

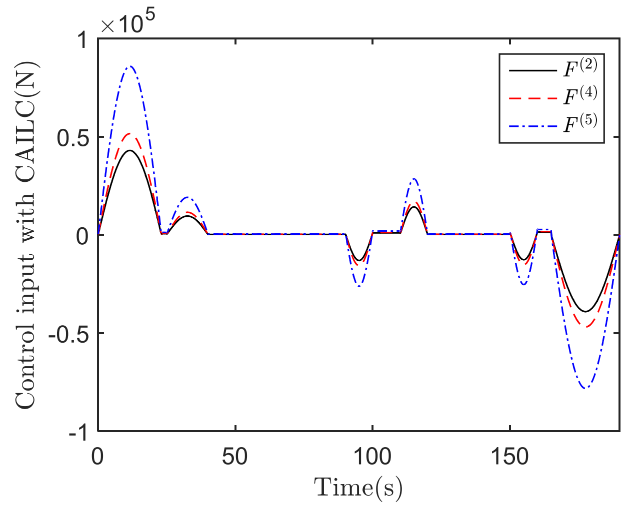

Fig. 9. Traction/Braking force contributed by motoring vehicles with the proposed CAILC.

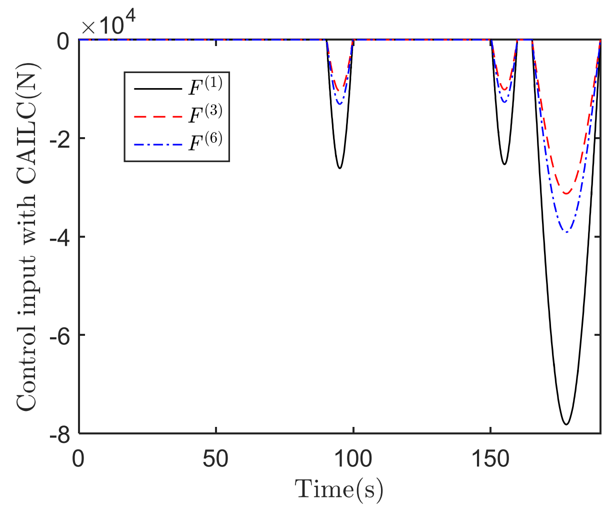

Fig. 10. Braking force contributed by trailers with the proposed CAILC.

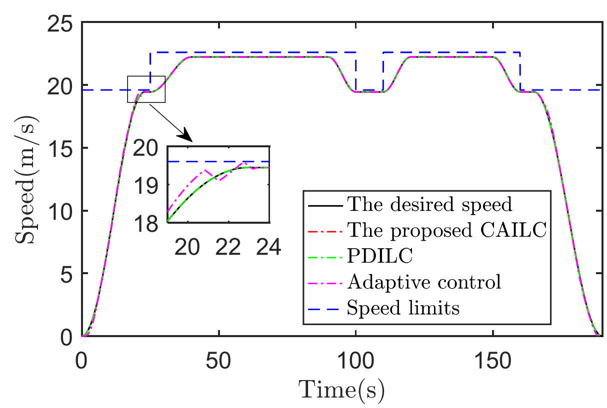

Fig. 11. Speed tracking profile with the proposed CAILC, PDILC and adaptive control at the 10th iteration under disturbance.

Considering the disturbance, system (9) can be rewritten as

$$M\ddot{x}_i(t) = \boldsymbol{\Upsilon} \boldsymbol{F}_i(t) + \boldsymbol{\Xi}^T(t)\boldsymbol{\xi}_i(t) + Md_i(t) \tag{65}$$

where $d_i(t)$ is the random load disturbance of magnitude $[-0.01, 0.01]$ on unit mass.

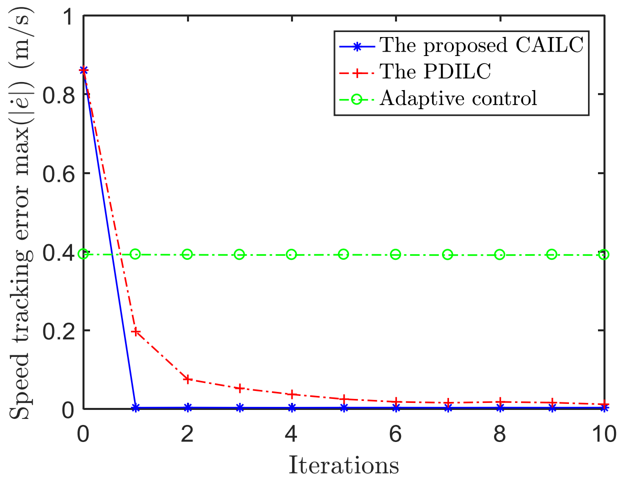

Fig. 12. The maximum speed tracking error with the proposed CAILC, PDILC and adaptive control under disturbance.

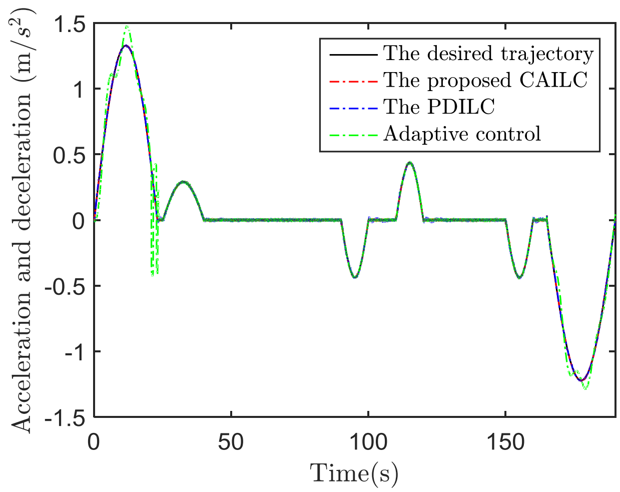

Fig. 13. Acceleration and deceleration profile with the proposed CAILC, PDILC and adaptive control under disturbance.

The simulation setup in this section is the same as example 1. Fig. 11 and Fig. 12 are the speed tracking profile and the maximum speed tracking error profile under the disturbance, respectively. Fig. 13 is the acceleration and deceleration profile. It is clear that in the case of disturbance, the proposed control algorithm can still ensure the safe and reliable operation of the subway train and meet control requirements.

VII. Conclusion

The subway train is a strong uncertain nonlinear system and consists of many vehicles. Hence, the multiple-point-mass dynamic model of subway train system can describe train system accurately than single-point-mass model. A novel adaptive iterative learning control algorithm (AILC) for the speed and position tracking control utilizing the multiple-point-mass dynamic model of the subway train is developed in this paper. A composite energy function technique is utilized to obtain tracking error asymptotic convergence in the iteration axis. Furthermore, for over speed, derailment and collision of the subway train, a speed constraint adaptive iterative learning control law is also investigated. Finally, to illustrate the effectiveness of theoretical studies, two simulation examples of the subway train are conducted. The simulations results in the proposed CAILC of the subway train are provided for train system to show the advantages and effectiveness of theoretical studies. In the future, we will study iteration-dependent train mass for subway train system control under adaptive learning control framework based on the train multiple-point-mass dynamic model.

References

[1] Y. Wang, Z. Yang, and J. Pang, "Statistical analysis of urban rail transit lines in 2017 China-Express delivery of annual report on urban rail transit V," *Urban Mass Transit*, vol. 21, no. 1, pp. 1–6, 2018.

[2] H. Dong, B. Ning, B. Cai, and Z. Hou, "Automatic train control system development and simulation for high-speed railways," *IEEE Circuits Syst. Mag.*, vol. 10, no. 2, pp. 6–18, May 2010.

[3] T. Tang and L. Huang, "A survey of control algorithm for automatic train operation," *J. China Railway Soc.*, vol. 25, no. 2, pp. 98–102, 2003.

[4] E. Khmelnitsky, "On an optimal control problem of train operation," *IEEE Trans. Autom. Control*, vol. 45, no. 7, pp. 1257–1266, Jul. 2000.

[5] Y. Bocharnikov, A. Tobias, C. Roberts, S. Hillmansen, and C. Goodman, "Optimal driving strategy for traction energy saving on DC suburban railways," *IET Electr. Power Appl.*, vol. 1, no. 5, pp. 675–682, Sep. 2007.

[6] S. Lu, S. Hillmansen, T. K. Ho, and C. Roberts, "Single-train trajectory optimization," *IEEE Trans. Intell. Transp. Syst.*, vol. 14, no. 2, pp. 743–750, Jun. 2013.

[7] Y. Wang, B. De Schutter, T. J. van den Boom, and B. Ning, "Optimal trajectory planning for trains–A pseudospectral method and a mixed integer linear programming approach," *Transp. Res. C, Emerg. Technol.*, vol. 29, pp. 97–114, Apr. 2013.

[8] S. Su, X. Li, T. Tang, and Z. Gao, "A subway train timetable optimization approach based on energy-efficient operation strategy," *IEEE Trans. Intell. Transp. Syst.*, vol. 14, no. 2, pp. 883–893, Jun. 2013.

[9] S. Su, T. Tang, X. Li, and Z. Gao, "Optimization of multitrain operations in a subway system," *IEEE Trans. Intell. Transp. Syst.*, vol. 15, no. 2, pp. 673–684, Apr. 2014.

[10] J. T. Haahr, D. Pisinger, and M. Sabbaghian, "A dynamic programming approach for optimizing train speed profiles with speed restrictions and passage points," *Transp. Res. B, Methodol.*, vol. 99, pp. 167–182, May 2017.

[11] S. H. Han, Y. S. Byen, J. H. Baek, T. K. An, S. G. Lee, and H. J. Park, "An optimal automatic train operation (ATO) control using genetic algorithms (GA)," in *Proc. IEEE Region Conf.*, Cheju Island, South Korea, Sep. 1999, pp. 360–362.

[12] J. Yin, D. Chen, and L. Li, "Intelligent train operation algorithms for subway by expert system and reinforcement learning," *IEEE Trans. Intell. Transp. Syst.*, vol. 15, no. 6, pp. 2561–2571, Dec. 2014.

[13] H. Liu, X. Zhang, and W. Chang, "PID control to maglev train system," in *Proc. Int. Conf. Ind. Inf. Syst.*, Apr. 2009, pp. 341–343.

[14] J. Yang, L. Jia, Y. Fu, and S. Lu, "Speed tracking based energy-efficient freight train control through multi-algorithms combination," *IEEE Intell. Transp. Syst. Mag.*, vol. 9, no. 2, pp. 76–90, Apr. 2017.

[15] H. Oshima, S. Yasunobu, and S.-I. Sekino, "Automatic train operation system based on predictive fuzzy control," in *Proc. Int. Workshop Artif. Intell. Ind. Appl.*, Jan. 2003, pp. 485–489.

[16] Y. Wang, R. Luo, Z. Yu, and B. Ning, "Study on ATO control algorithm with consideration of ATP speed limits," *J. China Railway Soc.*, vol. 34, no. 5, p. 17, 2012.

[17] F. Lu, M. Song, X. Li, and G. Tian, "Event-based control technology and the application in subway train operation," *China Railway Sci.*, vol. 27, no. 4, pp. 106–111, 2006.

[18] C. Dullinger, W. Struckl, and M. Kozek, "Simulation-based multi-objective system optimization of train traction systems," *Simul. Model. Pract. Theory*, vol. 72, pp. 104–117, Mar. 2017.

[19] J. Liu, H. Guo, and Y. Yu, "Research on the cooperative train control strategy to reduce energy consumption," *IEEE Trans. Intell. Transp. Syst.*, vol. 18, no. 5, pp. 1134–1142, May 2017.

[20] X.-G. Guo, J.-L. Wang, and F. Liao, "Adaptive fuzzy fault-tolerant control for multiple high-speed trains with proportional and integral-based sliding mode," *IET Control Theory Appl.*, vol. 11, no. 8, pp. 1234–1244, May 2017.

[21] X.-G. Guo, J.-L. Wang, F. Liao, and R. S. H. Teo, "CNN-based distributed adaptive control for vehicle-following Platoon with input saturation," *IEEE Trans. Intell. Transp. Syst.*, vol. 19, no. 10, pp. 3121–3132, Oct. 2018.

[22] X. Guo, J. Wang, F. Liao, and R. S. H. Teo, "Neuroadaptive quantized PID sliding-mode control for heterogeneous vehicular platoon with unknown actuator deadzone," *Int. J. Robust Nonlinear Control*, vol. 29, no. 1, pp. 188–208, 2019.

[23] A. Tayebi and C.-J. Chien, "A unified adaptive iterative learning control framework for uncertain nonlinear systems," *IEEE Trans. Autom. Control*, vol. 52, no. 10, pp. 1907–1913, Oct. 2007.

[24] J.-X. Xu, "A survey on iterative learning control for nonlinear systems," *Int. J. Control*, vol. 84, no. 7, pp. 1275–1294, Jul. 2011.

[25] X. Jin and J.-X. Xu, "Iterative learning control for output-constrained systems with both parametric and nonparametric uncertainties," *Automatica*, vol. 49, no. 8, pp. 2508–2516, Aug. 2013.

[26] D. Shen and Y. Wang, "Survey on stochastic iterative learning control," *J. Process Control*, vol. 24, no. 12, pp. 64–77, Dec. 2014.

[27] R. Zhang, Z. Hou, R. Chi, and H. Ji, "Adaptive iterative learning control for nonlinearly parameterised systems with unknown time-varying delays and input saturations," *Int. J. Control*, vol. 88, no. 6, pp. 1133–1141, Jun. 2015.

[28] Z. Hou, Y. Wang, C. Yin, and T. Tang, "Terminal iterative learning control based station stop control of a train," *Int. J. Control*, vol. 84, no. 7, pp. 1263–1274, Jul. 2011.

[29] H. Sun, Z. Hou, and D. Li, "Coordinated iterative learning control schemes for train trajectory tracking with overspeed protection," *IEEE Trans. Autom. Sci. Eng.*, vol. 10, no. 2, pp. 323–333, Apr. 2013.

[30] H. Ji, Z. Hou, and R. Zhang, "Adaptive iterative learning control for high-speed trains with unknown speed delays and input saturations," *IEEE Trans. Autom. Sci. Eng.*, vol. 13, no. 1, pp. 260–273, Jan. 2016.

[31] Q. Yu, Z. Hou, and J.-X. Xu, "D-type ILC based dynamic modeling and norm optimal ILC for high-speed trains," *IEEE Trans. Control Syst. Technol.*, vol. 26, no. 2, pp. 652–663, Mar. 2018.

[32] C.-D. Yang and Y.-P. Sun, "Mixed H_2/H cruise controller design for high speed train," *Int. J. Control*, vol. 74, no. 9, pp. 905–920, 2001.

[33] X. Zhuan and X. Xia, "Speed regulation with measured output feedback in the control of heavy haul trains," *Automatica*, vol. 44, no. 1, pp. 242–247, Jan. 2008.

[34] M. Ganesan, D. Ezhilarasi, and J. Benni, "Hybrid model reference adaptive second order sliding mode controller for automatic train operation," *IET Control Theory Appl.*, vol. 11, no. 8, pp. 1222–1233, May 2017.

[35] Q. Song, Y.-D. Song, T. Tang, and B. Ning, "Computationally inexpensive tracking control of high-speed trains with traction/braking saturation," *IEEE Trans. Intell. Transp. Syst.*, vol. 12, no. 4, pp. 1116–1125, Dec. 2011.

[36] Z. Li, Z. Hou, and C. Yin, "Iterative learning control for train trajectory tracking under speed constrains with iteration-varying parameter," *Trans. Inst. Meas. Control*, vol. 37, no. 4, pp. 485–493, Apr. 2015.

[37] H. K. Khalil, *Noninear Systems Third Edition*, 3rd ed. Upper Saddle River, NJ, USA: Prentice-Hall, 2002.

[38] J.-X. Xu and J. Xu, "On iterative learning from different tracking tasks in the presence of time-varying uncertainties," *IEEE Trans. Syst., Man, Cybern., B (Cybern.)*, vol. 34, no. 1, pp. 589–597, Feb. 2004.

[39] M. Sun and S. Ge, "Adaptive repetitive control for a class of nonlinearly parametrized systems," *IEEE Trans. Autom. Control*, vol. 51, no. 10, pp. 1684–1688, Oct. 2006.

[40] T. Tang, J. Xun, F. Cao, Y. Wang, and S. Su, "Research on energy-efficient driving strategy in Beijing Yizhuang line," *J. Beijing Jiaotong Univ.*, vol. 40, no. 4, pp. 19–24, Aug. 2016.

[41] Z. Rao, *Train Traction Calculation*. Beijing, China: China Railway, 2006.

[42] *Standard of Metro Gauges*, China Standard CJJ 96-2003, 2003.

[43] Z. Feng, Z. Zhang, and D. Pi, "Open-closed-loop pd-type iterative learning controller for nonlinear systems and its convergence," in *Proc. 5th World Congr. Intell. Control Autom.*, Nov. 2004, pp. 1241–1245.

[44] R. R. Liu and I. M. Golovitcher, "Energy-efficient operation of rail vehicles," *Transp. Res. A, Policy Pract.*, vol. 37, no. 10, pp. 917–932, Dec. 2003.

[45] *General Technical Specification for Metro Vehicles*, China Standard GB /T 7928-2003, 2003.

Genfeng Liu received the B.S. degree in electric engineering and automation and the M.S. degree in control science and engineering from Henan Polytechnic University, Jiaozuo, China, in 2012 and 2015, respectively. He is currently pursuing the Ph.D. degree in control science and engineering with the Advanced Control System Laboratory, School of Electronic and Information Engineering, Beijing Jiaotong University, Beijing, China.

His research interests include data-driven control, iterative learning control, model free adaptive control, adaptive control, fault-tolerant control, and train control systems.

Zhongsheng Hou (Fellow, IEEE) received the B.S. and M.S. degrees from the Jilin University of Technology, Jilin, China, in 1983 and 1988, respectively, and the Ph.D. degree from Northeastern University, Shenyang, China, in 1994.

From 1995 to 1997, he was a Post-Doctoral Fellow at the Harbin Institute of Technology, Harbin, China. From 2002 to 2003, he was a Visiting Scholar with Yale University, Yale, CT, USA. From 1997 to 2018, he was with Beijing Jiaotong University, Beijing, China, where he was a Distinguished Professor and the Founding Director of the Advanced Control Systems Lab, and the Head of the Department of Automatic Control. He is currently a Chair Professor with the School of Automation, Qingdao University, Qingdao, China. His research interests are in the fields of data-driven control, model-free adaptive control, learning control, and intelligent transportation systems. Until now, he has authored or coauthored more than 180 peer-reviewed journal articles and over 140 papers in prestigious conference proceedings. He has authored two monographs, Nonparametric Model and its Adaptive Control Theory (Science Press, 1999) (in Chinese), and Model Free Adaptive Control: Theory and Applications (CRC Press, 2013). His pioneering work on model-free adaptive control has been verified in more than 160 different field applications, laboratory equipment, and simulations with practical background, including wide-area power systems, lateral control of autonomous vehicles, and temperature control of silicon rod. His works on data-driven learning and control has been supported by multiple projects supported by the National Natural Science Foundation of China (NSFC), including three Key Projects in 2009, 2015, and 2019, respectively, and a Major International Cooperation Project in 2012.

Prof. Hou is the Founding Director of the Technical Committee on Data Driven Control, Learning and Optimization (DDCLO), the Chinese Association of Automation (CAA), and is a fellow of the CAA. He is also an International Federation of Automatic Control Technical Committee Member of both "Adaptive and Learning Systems" and "Transportation Systems." He was the Guest Editor for two Special Sections on the topic of data-driven control of the IEEE TRANSACTIONS ON NEURAL NETWORKS (2011), and the IEEE TRANSACTIONS ON INDUSTRIAL ELECTRONICS (2017).